Environmental Science and Pollution Research (2020) 27:43711–43723
https://doi.org/10.1007/s11356-020-10232-1

RESEARCH ARTICLE

Treatment of mixed dairy and dye wastewater in anode of microbial fuel cell with simultaneous electricity generation

Rana Tajdid Khajeh[1] · Soheil Aber[1] · Katayoon Nofouzi[2] · Sirous Ebrahimi[3]

Received: 29 February 2020 / Accepted: 20 July 2020 / Published online: 1 August 2020

Abstract

Microbial fuel cell (MFC) is a green technology that converts the stored chemical energy of organic matter to electricity; therefore, it can be used for wastewater purification and energy production simultaneously. In this study, three kinds of dairy products, including milk, cheese water, and yogurt water, were mixed with Acid orange 7 (AO7) as the model wastewater and used as the anolyte of an MFC. The capability of the system in energy production and dye removal was also investigated. The FESEM images were used to investigate the biofilms attachment to the anodes. Moreover, the polarization curves, electrochemical impedance spectroscopy, cyclic voltammetry (CV), voltage–time profiles, and coulombic efficiency were used to evaluate the electrochemical activity of the MFCs. Based on the CV results, the biofilm formation significantly improved the electrochemical activity of the electrodes. Maximum power density, voltage, and coulombic efficiency were obtained as 44.05 $mW.m^{-2}$, 332.4 mV, and 1.76%, respectively, for cheese water + AO7 anolyte, but the milk + AO7 MFC produced a stable voltage for a long time and its performance was similar to the cheese water + AO7 anolyte. Maximum COD removal and decolorization efficiencies were obtained equal to 84.57 and 92.18% for yogurt water + AO7 and cheese water + AO7 anolytes, respectively.

Keywords Acid orange7 · Bioenergy · Cheese · Milk · Yogurt

Highlights
- Azo dye decolorization in a MFC system using dairy products was studied for the first time.
- The produced biofilms were rich in microorganisms.
- Cheese water + AO7 and milk + AO7 as the anolytes of MFC had > 80% COD removal and > 90% decolorization efficiencies.
- It was shown that the type of anolyte has significant impression on the electrochemical activity.
- High power density and voltage output were achieved for cheese water + AO7 and milk + AO7 anolytes with long-time stable voltage.

Responsible Editor: Weiming Zhang

✉ Soheil Aber
soheil_aber@yahoo.com; s_aber@tabrizu.ac.ir

Rana Tajdid Khajeh
rana_tajdidkhajeh@yahoo.com

Katayoon Nofouzi
nofouzi@tabrizu.ac.ir

Sirous Ebrahimi
sirous.ebrahimi@epfl.ch

[1] Research Laboratory of Environmental Protection Technology, Department of Applied Chemistry, Faculty of Chemistry, University of Tabriz, Tabriz, Iran

[2] Faculty of Veterinary Medicine, University of Tabriz, Tabriz, Iran

[3] Department of Chemical Engineering, Sahand University of Technology, Tabriz, Iran

Introduction

Industrial development is vital for all societies, but it creates some challenges, e.g., high energy demand and wastewater production, which needs consideration (Miran et al. 2015; Ismail and Habeeb 2017; Hindatu et al. 2017). Nowadays, making industries independent of fossil fuels and treating wastewater for energy production are the most attended fields by researchers (Miran et al. 2016; Burkitt et al. 2016; Modi et al. 2016). Microbial fuel cell (MFC) is a green technology that not only treats wastewaters but also produces electricity via the catalytic activity of electroactive microorganisms, which releases the stored chemical energy of biodegradable organics (Liu et al. 2014; Miran et al. 2016; Garino et al. 2016). In MFC, the microorganisms in the anaerobic anodic chamber oxidize organic fuels via their metabolism. The produced electrons and protons in the anodic chamber are transferred to the cathodic chamber via an external circuit and a proton exchange membrane, respectively, and make it possible to reduce the electron acceptor in the cathodic chamber (Rikame et al. 2012; Wang et al. 2015; Huang et al. 2016; Penteado et al. 2017). Cell design; membrane type; the characteristics and structure of electrode materials; fuel, inoculated microorganisms, and electrolyte type; and temperature and pH are the most effective parameters in MFC performance (Cirik 2014; Jadhav et al. 2017). Glucose, sucrose, acetate, formate, oxalate, starch, etc. are the most used fuels in MFCs (Shin et al. 2014; Yuan et al. 2017); however, a complex matrix of compounds can be used as fuel in the anode chamber, too (Ge et al. 2014; Faria et al. 2017; Cao et al. 2017; Khan et al. 2017).

Leather, paper, textile, dying, dye manufacturing, and other industries use or produce synthetic dyes and discard a considerable amount of dyes as wastewater in the environment (Holkar et al. 2016). Dye wastewater contains chemicals which are harmful and toxic for the ecosystem, human being, animals, and plants; and as a consequence, disposing of them without enough treatment is unacceptable. It is hard to treat the dye wastewater due to its complicated and stable aromatic and heterocyclic components (Holkar et al. 2016, 2018; Katheresan et al. 2018). The physical, chemical, and biological processes are known as dye treatment methods. Adsorption and membrane filtration processes including nano-filtration, ultra-filtration, and reverse osmosis are examples of physical methods. The high price of membranes and some adsorbents, not degrading pollutants in adsorption methods, and converting the adsorbent to waste are the main disadvantages of the physical processes. The advanced oxidation, ozonation, electrochemical, and photochemical processes are some known chemical dye removal methods. These methods require high electrical energy and specific equipment with high consumption of chemical reagents; therefore, they are not practical for large-scale applications (Jegatheesan et al. 2016; Holkar et al. 2016; Katheresan et al. 2018). Biological methods are cheap and can be performed on large scales. Therefore, the biological treatment processes are preferred. The aerobic biological processes are not applicable to the treatment of high chemical oxygen demand (COD) and organic contents due to high energy requirements and high amounts of sludge production. However, the anaerobic processes are capable of reducing high COD values, while they produce low amounts of sludge (Karadag et al. 2015a, b; Su et al. 2016).

Dairy industries produce large amounts of wastewater containing high organic loading with high biological oxygen demand (BOD) and COD values. Carbohydrates, fats, and proteins are the major components of dairy effluents. While they cause problems for the environment and treatment plants due to high organic content, their energy can be reused and recovered (Hassan and Nelson 2012; Karadag et al. 2015a). The MFCs can be used in order to harvest the energy from wastewater (Table 1).

As literature review shows, many researches have been devoted to promote MFC performance using co-substrates; however, to the best of our knowledge, the azo dye removal using MFC systems in the presence of dairy products has not been studied yet. The high organic content of dairy wastewater is a suitable carbon source for anaerobic biofilm in the anodic chamber of MFC and can help in dye removal.

The aim of this study was to replace the usual nutritional agents with a waste by-product (dairy wastewater) in an MFC, which treats AO7 wastewater. The dye and dairy wastewater are not available in mixed condition, but if the mixed wastewater shows promising results, it is worth to transfer the dairy wastewater to the MFC system. In this research, the effects of the application of various mixtures of AO7 and dairy products (milk, cheese water, and yogurt water) as feed in the anodic chamber of an MFC were investigated. AO7 decolorization, COD removal efficiency, and voltage and power density generation using different feed mixtures were monitored and the developed biofilm structure was also studied.

Materials and methods

Microorganism adaptation and biofilm formation on the graphite anode electrode

AO7 (Alvan Sabet, Hamedan, Iran) is toxic (Fernando et al. 2012, 2014a), requiring the adaptation of microorganisms to the dye before application as a substrate in the anolyte of MFC. In this study, an adaptation period of 14 days was performed in a container. A total volume of 200 ml of anolyte containing 1% (*v*/*v*) of one of the dairy products (milk, cheese water, and yogurt water) and 5% (*v*/*v*) anaerobic activated sludge from the wastewater treatment plant of East Azarbaijan Pegah Pasteurized Milk Co. in Tabriz, Iran, was

Table 1 The literature review to compare the decolorization efficiency and maximum power density of MFC systems

MFC system	Dye	Co-substrate	Decolorization	Power density	Reference
Air-cathode microbial fuel cells	Congo Red	Glucose	Complete decolorization	58 $mW.m^{-2}$	(Sun et al. 2015)
H-type MFCs	Acid orange 7 (AO7)	Sodium pyruvate and sodium acetate	98%	39.2 $mW.m^{-2}$	(Fernando et al. 2012)
Dual chamber MFC	Acid Red 27	Glucose	98%	458.8 $mW.m^{-2}$	(Kardi et al. 2016)
Dual chamber MFC	Direct Red 80	Ethanol	75%	269 $mW.m^{-2}$	(Miran et al. 2015)
Integrated cylindrical single chamber MFCs and aerobic bioreactor system	Acid Red 27	Molasses	Complete decolorization	51.9 $mW.m^{-2}$	(Fernando et al. 2014a)
Two-chamber microbial fuel cell	Reactive Blue-19	Glucose	90%	84 $mW.m^{-2}$	(Holkar et al. 2018)

filled in a glass container, then the graphite electrode was immersed in this solution for 48 h while stirring. After that, the anolyte was replaced with a new one containing 1 ppm dye, 1% (*v*/*v*) dairy product, and 5% (*v*/*v*) anaerobic activated sludge. This replacement was performed every 48 h with increasing AO7 concentration in each replacement (1, 5, 15, 50, and 100 ppm), while the concentrations of the other components were constant. During the adaptation period, the system was purged by N_2 gas for 15 min after filling the container with the anolyte in order to provide the anaerobic conditions.

MFC configuration and operation

MFC setup was made of Plexiglas containing two chambers that were separated with a Nafion N966 membrane. The volume of each chamber was 700 mL. Anode chamber was kept in anaerobic condition and it was filled with the anolyte containing K_2HPO_4/KH_2PO_4 (50 mM) buffer solution, $MgSO_4$ 0.02 $g.L^{-1}$, NH_4Cl 0.38 $g.L^{-1}$, NaCl 0.5 $g.L^{-1}$, $KHCO_3$ 2 $g.L^{-1}$, and $CuCl_2$ 0.003 $g.L^{-1}$, and all of the mentioned chemicals were analytical grade from Merck, Germany. Anode chamber was purged with N_2 gas for 20 min before starting the experiments to provide anaerobic conditions. The dairy product (yogurt water, milk, cheese water) and AO7 were added to the anolyte repeatedly when the voltage of the MFC decreased below 60 mV. Cathode chamber was filled with K_2HPO_4/KH_2PO_4 (50 mM) buffer solution. An air pump (pumping rate = 1 $L.min^{-1}$) was used to enter O_2 as an electron acceptor in the catholyte.

Graphite plates (5 cm × 5 cm) were used as anode and cathode electrodes. Copper wire was used to connect the anode and the cathode, and a resistor box was used to set the external resistance at 500 Ω unless otherwise mentioned. The distance between the anode and the cathode electrodes was fixed at 6 cm and the temperature was fixed at 35 ± 2 °C in an incubator assembled in our laboratory. The schematic diagram of the MFC system is illustrated in Fig. 1.

Analyses

The potential of the MFC was measured at time intervals of 5 min using a digital multimeter (VICTOR 86D, China). The concentration of AO7 was determined by a UV–Vis spectrophotometer (T80+; PG Instrument Limited, UK) and COD of the anode solution was measured according to the 5220D standard method (Rice et al. 2017). COD measurements were performed in duplicate.

FESEM analysis

The morphology of the biofilm formed on the anode was characterized by field scanning electron microscopy (MIRA3 FE-SEM, Tescan, and Czech). Before the FESEM analysis, the biofilm samples were pretreated. For pretreatment, the biofilm samples were immersed in 10 and 5% glutaraldehyde solutions, each for 8 h, respectively, and then dehydrated by submerging them in 30, 50, and 96% ethanol

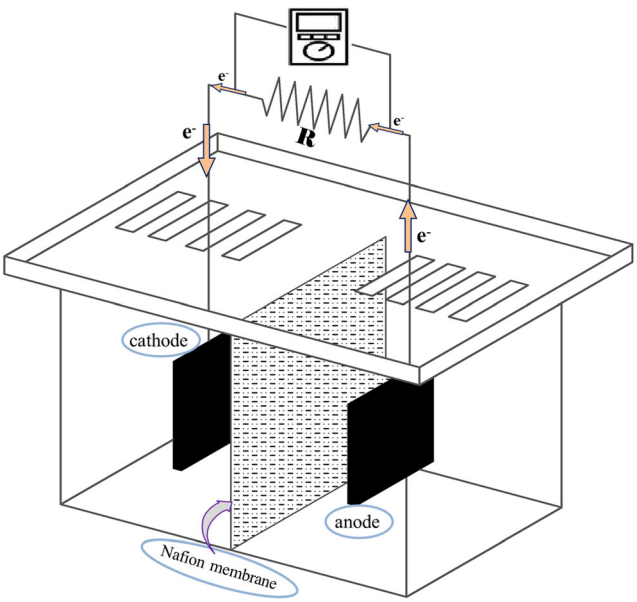

Fig. 1 Schematic diagram of the two-chamber microbial fuel cell setup

solutions, each for 15 min, respectively (Wang et al. 2017; Chen et al. 2018).

Cyclic voltammetry (CV) and electrochemical impedance spectroscopy (EIS)

Cyclic voltammetry was performed using an AUTOLAB/PGSTAT100 Metrohm device to investigate the electrochemical activity of the electrodes in a K_2HPO_4/KH_2PO_4 (50 mM) buffer solution, and also in the MFC system at the voltage range of − 1 to 1 V and a scan rate of 10 $mV.s^{-1}$. A three-electrode system including a standard calomel reference (SCE) electrode, a platinum counter electrode, and a biofilm-coated working electrode was employed for CV analyses in the buffer solution (Liu et al. 2014). In the CV analyses which were performed in the MFC system, the SCE, cathode, and anode of the MFC were set as the reference, counter, and working electrodes, respectively, while the SCE was placed between the anode electrode and membrane (Chen et al. 2018).

An IviumStat potentiostat/galvanostat was used for EIS analyses with Ag/AgCl (reference), platinum (counter), and biofilm-coated (working) electrodes. EIS was performed in two different electrolytes, first in a 10 mM $K_3[Fe(CN)_6]/K_4[Fe(CN)_6]$ + 0.1 M KCl electrolyte and then in MFC's anolyte solution at 0.01–100 kHz frequency range and a potential amplitude of 10 mV (Chen et al. 2018).

Calculation of chemical and electrochemical parameters

Calculation of decolorization efficiency

Decolorization efficiency is an important parameter to evaluate the performance of those MFC systems which treat the colored wastewaters. For this purpose, the absorbance of the anolyte was measured by the UV–Vis spectrophotometer at 484 nm (Fernando et al. 2014a; Abdollahi et al. 2018) and the corresponding dye concentration was calculated using the corresponding calibration curve. Eventually, decolorization efficiency was calculated using Eq. 1, where c_0 and c are the initial and final concentrations of AO7, respectively.

$$\mathrm{R}\ (\%) = \left(\frac{\mathbf{C_0}-\mathbf{C}}{\mathbf{C_0}}\right) \times 100 \tag{1}$$

Power density

The power density of an MFC system specifies its capability in electrical energy production. In this work, different external resistances (10,000 to 10 Ω) were set in the external circuit when the maximum and stable voltage of the MFC system was achieved, then the voltage was measured by the multimeter to calculate the current and power density. Current and power densities were calculated according to Eqs. 2 and 3 where I, V, R, P, and A are current (A), voltage (V), resistance (Ω), power density ($W.m^{-2}$), and anode surface area (m^2), respectively.

$$I = \frac{V}{R} \tag{2}$$

$$P = \frac{I \times V}{A} \tag{3}$$

Coulombic efficiency (CE)

Equation 4 was used to calculate the coulombic efficiency, where M, I, b, F, V, t, and ΔCOD are molecular weight, current (A), number of electrons participating in the reaction, Faraday's constant (96,485 $C.mol^{-1}$), anolyte volume (L), time, and difference between initial COD and the COD in a specific time (t) ($g.L^{-1}$), respectively.

$$\mathrm{CE}\ (\%) = \frac{M \int_0^t I\ \mathrm{d}t}{b\ F\ V\ \Delta\mathrm{COD}} \times 100 \tag{4}$$

Results and discussion

FESEM analyses of biofilm on the graphite plate electrode

Milk consists of water, lipids, carbohydrates, proteins, salts, vitamins, and a large number of other constituents. The composition of milk changes during the coagulation processes of the production of cheese and yogurt. Some proteins, e.g., casein are coagulated, while the water-soluble proteins, constituting one fifth of the total proteins of milk, remain soluble in water. The fat and fat-soluble vitamins are concentrated in the coagulated part and water-soluble vitamins and minerals remain in the remaining water. The compositions of milk, the coagulated part, and the uncoagulated part are different (Wong 1988); consequently, it is expected to observe different results with regard to the biofilm composition and its performance in the MFCs with cheese water + AO7, yogurt water + AO7, and milk + AO7 as the constituents of anolyte.

The presence of biofilm on the anode of MFC is vital and must be proved. FESEM was used for investigating the formation of biofilm and its morphology. FESEM images were prepared from the biofilm samples at the end of the adaptation stage and before starting the MFC experiments. Figure 2 shows the FESEM images of the biofilm-coated graphite plates and also the bare graphite. As shown in Fig. 2b–d, the dense biofilm layers covered the whole anode surfaces and

showed highly complicated structures composed of morphologically different cells. These cells adhered to each other and were frequently embedded within a self-produced matrix of extracellular polymeric substances (EPS) that transformed into an effective biofilm. EPSs are high molecular weight compounds covered by microorganisms and have a significant effect on the physicochemical properties including electron transfer. Different sizes and shapes of bacteria were spread out on the electrode surface. Some rod-shaped cells and also some loose clumps are noticeable on the electrode. According to Kim et al. (2006) these clumps include the bacteria that are able to ferment the complex substrates and break them down to smaller products. These products can then be used as substrates for electrochemically active bacteria within the biofilm to generate electricity (Kim et al. 2004).

MFC performance in electrical energy production and electrochemical activity

The maximum stable voltage, power density, and the time length that the maximum voltage was stable were the parameters used to study the capability of the mixed dairy + AO7 solutions to produce electricity. The voltage–time profiles of different anolytes are illustrated in Fig. 3. In this study, the initial dye and COD concentrations in the MFC systems were 150 and 2000 ppm O_2, respectively.

According to Fig. 3, all the voltage–time profiles consist of three steps in each cycle, starting after the feeding of the system. At the first step, the voltage increased gradually to the maximum value due to the abundance of feed for the microorganisms. The stable maximum voltage appears in the second step and the duration of this step is an important parameter in the performance of the system. The voltage-decreasing phase was the last step. This step was due to the decrease in the available nutrients and the increase in the number of microorganisms that need more feed (Zhao et al. 2017). The maximum voltage values of 274.9 mV (109.96 $mA.m^{-2}$) and 325.3 mV (130.12 $mA.m^{-2}$); 112.2 mV (44.88 $mA.m^{-2}$), 154.1 mV (61.64 $mA.m^{-2}$), and 175.5 mV (70.2 $mA.m^{-2}$); and 248.7 mV (99.48 $mA.m^{-2}$) and 332.4 mV (132.96 $mA.m^{-2}$) were achieved for milk + AO7, yogurt water + AO7, and cheese water + AO7 anolytes, respectively. The duration of maximum voltage is one of the main parameters which can be used for the comparison of MFC systems. The period in which the voltage was between the maximum voltage and 10% less than it was considered as the duration of

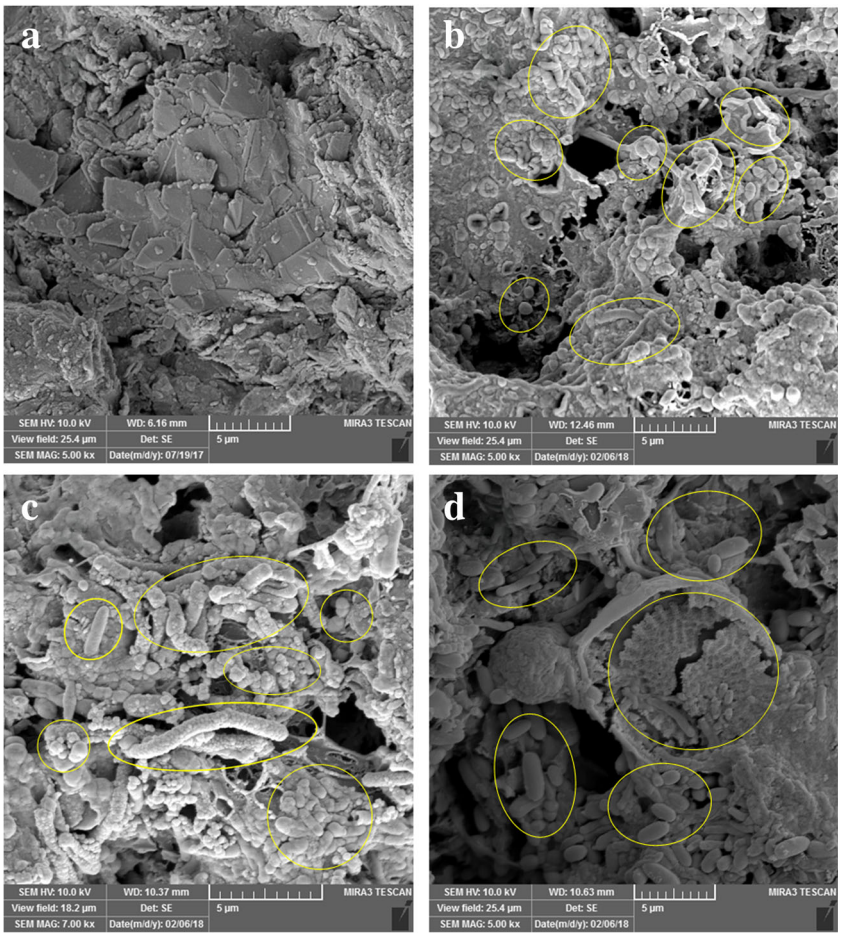

Fig. 2 FESEM image of **a** bare graphite, **b** biofilm of graphite in milk + AO7, **c** biofilm of graphite in cheese water + AO7, **d** biofilm of graphite in yogurt water + AO7

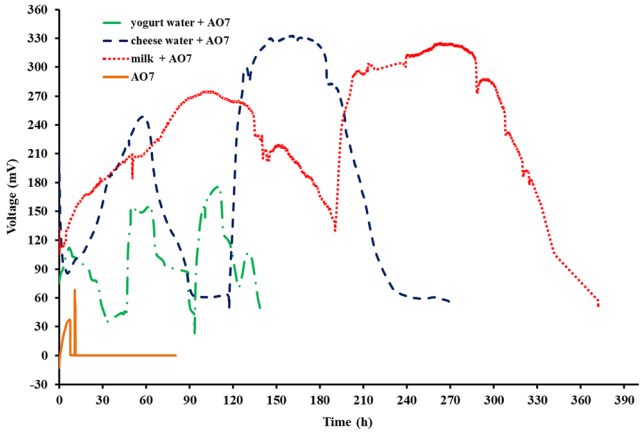

Fig. 3 Voltage–time profile of MFCs with three different kinds of feed in the anode chamber. Initial dye concentration = 150 ppm, initial COD = 2000 ppm O_2, electrode distance = 6 cm, and external resistance = 500 Ω

the maximum voltage. This period was from 77.5 to 134.5 h (57 h) for the first cycle and from 203 to 287 h (84 h) for the second cycle of milk + AO7 MFC. For the three cycles of yogurt water + AO7 MFC, the mentioned periods were in the ranges of 4.4–10.4 h (6 h), 48.5–65.5 h (17 h), and 101–112 h (11 h), respectively. In the first and second cycles of cheese water + AO7 MFC, the maximum voltage duration were from 48.4 to 63.4 h (15 h) and 133 to 188.7 h (55.7 h), respectively. According to the obtained results, milk + AO7 and cheese water + AO7 MFCs had the highest output voltage, while milk + AO7 MFC had the most long-term stable maximum voltage. Degradation of the dye and dairy products to the more biodegradable and digestible materials kept the voltage at a maximum level and created a nearly stable maximum voltage for a long time. Choi et al. (2007) investigated the effect of different simple carbon sources such as glucose, acetate, fructose, and lactose on the performance of MFC, whose results showed that the maximum voltages were

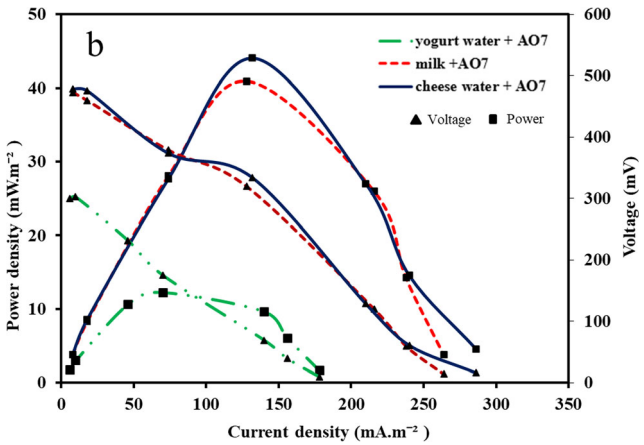

Fig. 4 Polarization and power density curves of MFCs with different kinds of anolyte. Initial dye concentration = 150 ppm, initial COD = 2000 ppm O_2, electrode distance = 6 cm at different external resistances (left *Y*- and right *Y*-axes correspond to power density and voltage, respectively)

stable for less than 2 h. Varanasi et al. (2016) used sodium acetate as a carbon source with the cycle time of 48 h and a stable maximum voltage period shorter than 48 h. Hence, the obtained stable maximum voltage periods in this study were significantly longer than those mentioned previously. According to Fig. 3, it is obvious that the application of AO7-only anolyte produced a negligible amount of voltage. This highlights the important role of the dairy by-products in the enhancement of electrical energy production in MFCs. In the previous work, the maximum voltage for an H-type MFC with pyruvate (1 $g.L^{-1}$) + casein hydrolysate (500 $mg.L^{-1}$) + AO7 (150 $mg.L^{-1}$) as the carbon source was 250 mV (Mani et al. 2017a). Venkata Mohan et al. (2010) investigated the power generation from dairy wastewater in a single chamber MFC at continuous mode and obtained a maximum voltage of 308 mV in the loading of 4.44 kg COD/m^3.

Power density and polarization curves

Power density and polarization curves are used to evaluate the performance of MFC systems. The polarization curve is a plot that shows voltage changes versus current density data. These data are obtained by changing the external resistance values from the infinite to low amounts producing certain voltage and current outputs at each resistance quantity (Logan 2008). The polarization curve consists of three parts. The first part appears in the low current density region due to the charge transfer overpotential. The second region relates to the ohmic voltage losses occurring slowly and is linear in most of the cases. The third part of the polarization curve refers to the mass transfer overpotential and concentration polarization (Logan et al. 2006; Zhao et al. 2009). The obtained results for this study are illustrated in Fig. 4 in which the polarization curves with three parts are obvious. According to Fig. 4, the power densities of 40.93 $mW.m^{-2}$ in 128 $mA.m^{-2}$, 44.04 $mW.m^{-2}$ in 132 $mA.m^{-2}$, and 12.26 $mW.m^{-2}$ in 70 $mA.m^{-2}$ were achieved for MFCs with milk + AO7, cheese water + AO7, and yogurt water + AO7, respectively. Therefore, milk and cheese produced higher power densities. The maximum power density for AO7 decolorization in the presence of different co-substrates was investigated by Fernando et al. (2012) and a 300-$mg.L^{-1}$ corn-steep liquor had the maximum power density equal to 19.28 $mW.m^{-2}$ for 195 $mg.L^{-1}$ of dye. Lai et al. (2017) investigated the decolorization of AO7 in a single chamber MFC with the laccase-producing white-rot fungus. Here, the produced laccase had the role of co-substrate, and the maximum power and current densities were 13.38 $mW.m^{-2}$ and 33 $mA.m^{-2}$, respectively. Therefore, the obtained results in our investigation showed that the power density of the MFCs with dairy products and AO7 had good performance compared with the literature (Table 2). The stable output power in a wide range of current density in the yogurt water + AO7 MFC system can be due to dominant

Table 2 The comparison of the maximum power density of different carbon source in MFCs

MFC system	Anode	Cathode	Carbon source	Dye	Temperature	pH	Microorganisms	Membrane	Power density	Reference
Two-chamber	Carbon cloth	Carbon cloth with Pt catalyst layer	Corn-steep liquor	AO7	–	7.0	*Shewanella oneidensis*	CMI-7000	19.3 $mW.m^{-2}$	(Fernando et al. 2012)
Two-chamber	Carbon fiber	Carbon fiber	Casein hydrolysate and pyruvate	AO7	30 °C	Anolyte pH = 7 Catholyte pH = 4.5	*Shewanella oneidensis*	Nafion 117	16 $mW.m^{-2}$	(Mani et al. 2017b)
Two-chamber	Graphite brush	Graphite bar	Glucose	Reactive Blue 221 (RB221)	29 ± 2 °C	7.0	Sludge	Nafion 117	20.2 $mW.m^{-2}$	(Savizi et al. 2012)
Single-chamber	Graphite rod	Stainless steel ring and activated carbon fiber (ACF)	Glucose	Reactive Brilliant Red X-3B	–	–	–	–	0.257 $W.m^{-3}$	(Cao et al. 2017)
Single-chamber	Carbon felt	Air cathode	Laccase	AO7	–	–	Anaerobic sludge	–	13.38 $mW.m^{-2}$	(Lai et al. 2017)
Two-chamber	Carbon paper	Carbon paper	Winery wastewater	–	20 ± 3 °C	6.5	Activated sludge	Sterion	8.37×10^{-6} $mW.m^{-2}$	(Penteado et al. 2017)
	carbon cloth	carbon cloth							0.76 $mW.m^{-2}$	
	carbon felt	carbon felt							420 $mW.m^{-2}$	
Two-chamber	Carbon cloth	VITO-CoRE™ cold-rolled gas diffusion electrodes (GDEs)	Sodium acetate	–	17 ± 1 °C	–	Manure	Zirfon®	0.75 $mW.m^{-2}$	(Pasupuleti et al. 2016)
Two-chamber	Graphite	Graphite	AO7 + cheese water	AO7	35 ± 2 °C	7	Anaerobic activated sludge	Nafion N966	44.04 $mW.m^{-2}$	This study

Table 3 Comparison of MFC results using different anolytes

Anolyte type	Cycle	Cycle time (h)	COD removal efficiency (%)	Decolorization efficiency (%)	CE (%)
Yogurt water + AO7	First cycle	46.75	84.56	77.13	0.21
	Second cycle	46.25	56.66	85.13	0.46
Milk + AO7	First cycle	187	81.76	91.66	1.7
	Second cycle	185	80.86	91.62	1.50
Cheese water + AO7	First cycle	117.17	72.84	92.18	1.25
	Second cycle	156.67	71.05	88.12	1.76

Initial dye concentration = 150 ppm, initial COD = 2000 ppm O_2, electrode distance = 6 cm, and external resistance = 500 Ω

ohmic resistance and low ionic conductivity of substance. The nonlinear state as can be seen in the polarization curve of cheese water + AO7 may be caused by the current independent parameters and electrode overpotentials beside the ohmic resistance (Logan et al. 2006).

Coulombic efficiency

Coulombic efficiency in MFC systems is a parameter expressing the ratio of the coulombs transferred to the anode to the total coulombs produced as a result of the oxidation of the substrates (Logan 2008; Hassan et al. 2017). The side reactions consume some of the electrons and prevent transferring those electrons from an external circuit; therefore, just some parts of the total coulombs take part in the current production (Mani et al. 2017a).The coulombic efficiencies calculated for different anolytes in this work are reported in Table 3. The maximum coulombic efficiencies of milk + AO7 and cheese water + AO7 MFCs were equal to 1.7 and 1.76%, respectively, which are comparable with and even better than those reported for dye + pyruvate + casein hydrolysate (1.13%) and dye + glucose (0.501%) (Fang et al. 2017; Mani et al. 2017a).

MFC performance in wastewater treatment

COD removal and decolorization efficiency

COD removal and decolorization efficiencies are two important parameters for evaluating the capability of the MFC systems which treat the colored wastewaters. The mechanism of the azo dye biodegradation and the MFC operation remains vague, unclear, and unexplored. The output voltage and AO7 decolorization can be affected with several anaerobic microbial activities including methanogenesis, fermentation, and denitrification, while the AO7 decolorization and electricity production compete with the other microbial activities in the electron consumption (Fernando et al. 2012; Thung et al. 2018). The highly charged AO7 structure and its large molecular size prevent the penetrating the dye molecules into the non-polar cell membrane of microorganisms; therefore, the extracellular electron transfer mechanism takes place for reductive destruction of the azo bond (–N=N–) of AO7 (Fernando et al. 2012, 2014b; Thung et al. 2018). This mechanism results in a negligible AO7 decolorization. When the dairy co-substrates are added, they act as electron donors for AO7 reduction. During AO7 reduction (Eq. 5) some intermediate compounds, e.g., sulfanilic acid and 1-amino 2-naphthol, are produced (Chen et al. 2010; Fernando et al. 2012, 2014b; Galai et al. 2015) that can act as the electron carriers to accelerate the decolorization and bioelectricity generation (Hsueh et al. 2014).

$$\mathrm{R{-}N=N{-}R\ddot{\epsilon} + 4\,e^- + 4\,H^+ \rightarrow R{-}NH_2 + R\ddot{\epsilon}{-}NH_2} \quad (5)$$

Figure 5 and Table 3 show COD removal and decolorization efficiencies of the first and the second cycles of the MFC. Maximum COD removal was 84.56% in the yogurt + AO7 MFC and maximum decolorization efficiency was 93.65% for milk + AO7 MFC. In all the cases, more than 75% decolorization and 55% COD removal efficiencies were attained. The COD removal and decolorization efficiencies of 72.84

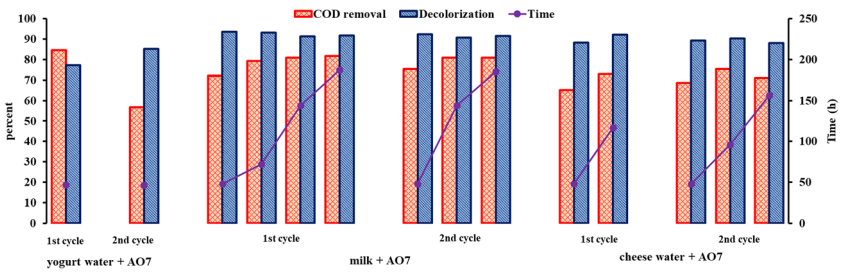

Fig. 5 COD removal and decolorization efficiency in different cycles of MFCs with different anolytes. Initial dye concentration = 150 ppm, initial COD = 2000 ppm O_2, electrode distance = 6 cm, and external resistance = 500 Ω

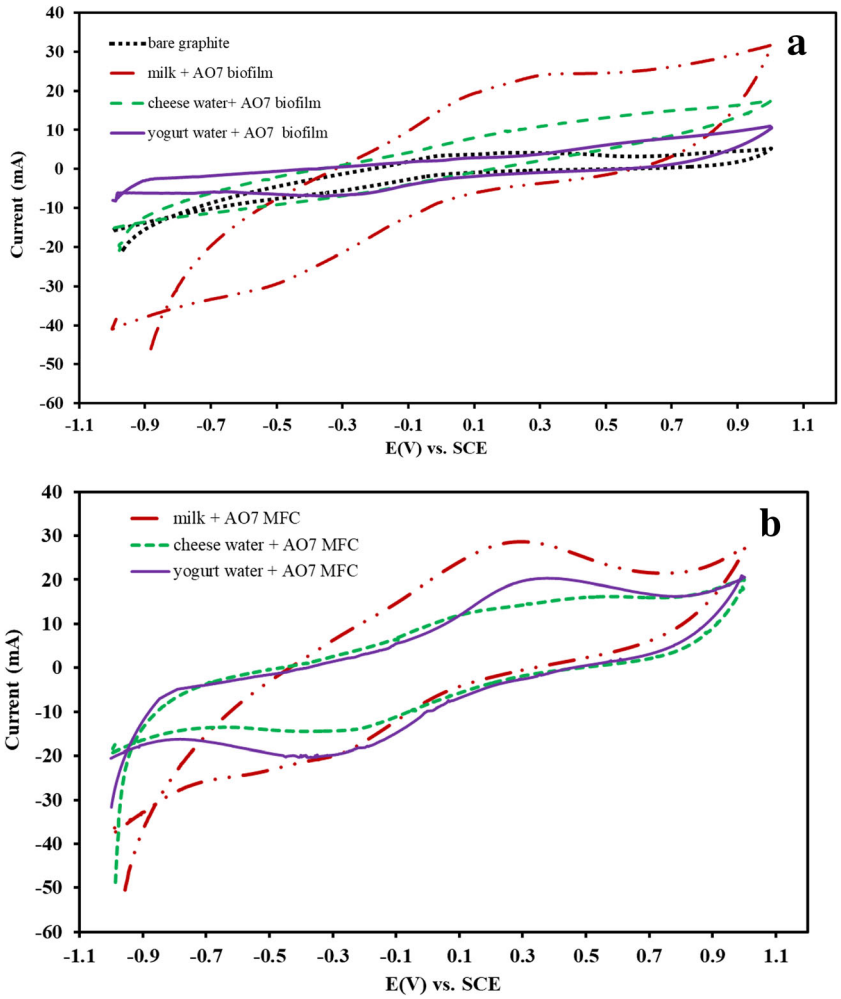

Fig. 6 Cyclic voltammograms of (**a**) bare graphite and different biofilm-coated electrodes as a working electrode, Pt as a counter electrode, and SCE as a reference electrode with the scan rate of 10 $mV.s^{-1}$ in a 50 mM K_2HPO_4/KH_2 PO_4 buffer solution; electrodes picked up at the end of the adaptation processes. (**b**) Anodes of different MFC anolytes. Anode and cathode of MFC as working and counter electrodes, respectively, and SCE as a reference electrode at the scan rate of 10 $mV.s^{-1}$, electrodes picked up at the end of the last cycle of MFC experiments

and 92.18% for cheese water + AO7 MFC indicate its good performance. The dairy wastewater or anolyte components may have absorbance interferences with AO7. As a result, the real AO7 decolorization efficiency is more than that was reported. In other words, we reported the least probable decolorization efficiency. In an MFC with an anolyte constituting solely from AO7, only 20% of decolorization was achieved after 80 h showing the important role of the dairy by-products in the enhancement of decolorization efficiency. The decolorization efficiency was stable during two cycles, especially for milk and cheese water + AO7 MFCs. Fernando et al. (2012) obtained the decolorization and COD removal efficiencies of 98 and 73.7%, respectively, for an AO7 solution (350 $mg.L^{-1}$) in the presence of 500 $mg.L^{-1}$ casein hydrolysate and 20 mM sodium pyruvate.

Cyclic voltammetry

Cyclic voltammetry is an electrochemical analysis that can be applied to investigate the electrocatalytic activity of electrodes. In this study, it was used to evaluate the electrochemical activity of two series of biofilm-coated electrodes; one series was obtained at the end of the adaptation processes, and the second series was obtained at the end of the last cycle of MFC experiments (Fig. 6a, b). According to Fig. 6a, there are no significant redox peaks in the voltammograms; however, the biofilm-coated electrodes showed higher current values, confirming that the formation of the biofilm on the electrodes improved its electrochemical activity. Samsudeen et al. (2015) investigated the performance of a plain graphite plate in the absence and presence of biofilm by cyclic voltammetry. The appearance of redox peaks in voltammograms of the biofilm-coated electrode confirmed its higher electrochemical activity compared with the bare graphite electrode. The biofilm-coated anode in milk + AO7 anolyte presented the most strong redox peak and the highest current value, perhaps it is due to the extracellular electron transfer by the microorganisms of the biofilm (Harnisch and Freguia 2012; Samsudeen et al. 2015), and the membrane-bound cytochromes that transfer electrons across the membrane from the inside of the microbial cell membrane to its outside (Schröder 2007; Islam et al. 2018). Figure 6b

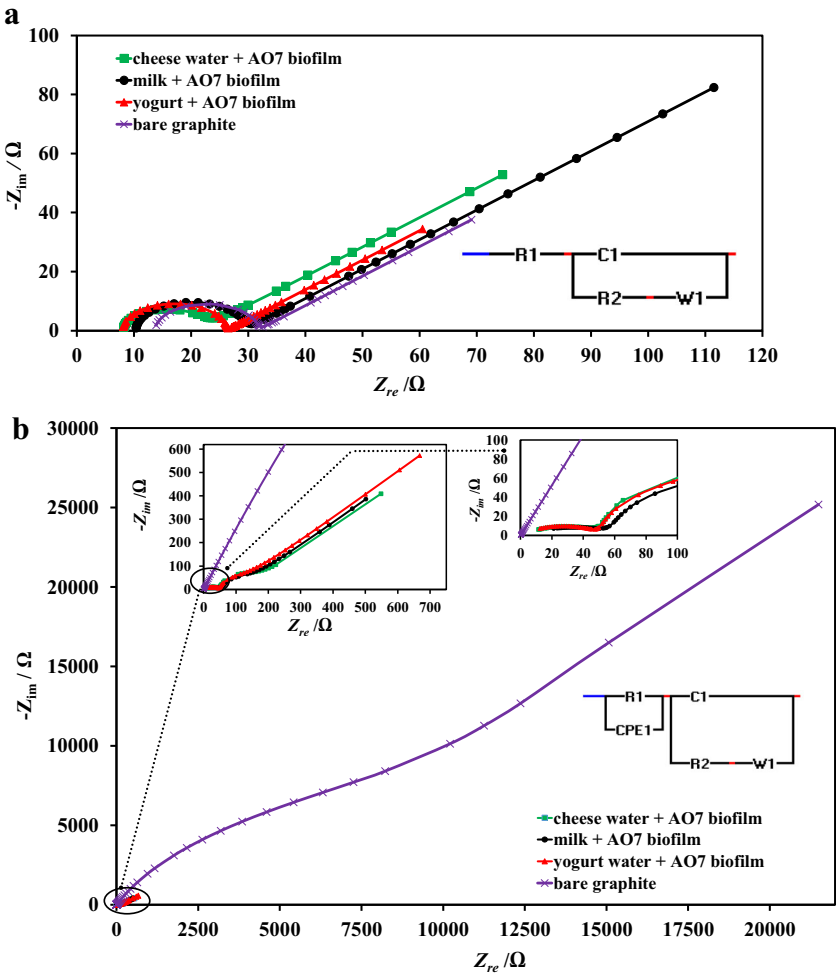

Fig. 7 Nyquist plots and the equivalent circuits of bare graphite and biofilm-coated electrodes in 0.01–100 kHz frequency range: **a** 10 mM $K_3[Fe(CN)_6]$/$K_4[Fe(CN)_6]$ + 0.1 M KCl solution; **b** anolyte solution

illustrates the voltammograms of the anodes that were obtained at the end of the last cycle of the MFC experiments. The redox peaks are obvious for yogurt water + AO7 and milk + AO7 MFCs, while they have higher current values, too. The presence of the substrates, extracellular matrix, formation of reversible redox couples, and the presence of mediators that are reversibly oxidized and reduced during CV tests create redox peaks (Harnisch and Freguia 2012; Islam et al. 2018). In a research with a biofilm-coated graphite felt and a platinum-coated graphite cloth as the anode and the cathode of a dual chamber MFC, respectively, they were used for the decolorization of Direct Red 80 in the presence of brewery wastewater (Miran et al. 2015), and the obtained maximum currents in the cyclic voltammetry tests were less than 10 and − 5 mA, while the values obtained in our work were 30 and − 20 mA for the milk + AO7 anolyte.

Electrochemical impedance spectroscopy

EIS helps to get important information about the voltage losses due to the ohmic (solution) resistance (R_s), charge transfer resistance (R_{ct}), and Warburg resistance (W) in the electrochemical systems. Generally, the impedance spectrum of an electrochemical system can be presented as a Nyquist plot. In

Table 4 EIS results of bare graphite and biofilm-coated electrodes in 0.01–100 kHz frequency range

MFC system	$K_3[Fe(CN)_6]/K_4[Fe(CN)_6]$ + 0.1 M KCl solution			Anolyte solution		
	R_1 (Ω)	R_2 (Ω)	W_1 (Ω)	R_1 (Ω)	R_2 (Ω)	W_1 (Ω)
Bare graphite	13.7	17.804	26.63	13,472	35,890	6052.2
Yogurt water + AO7	8.0439	18.07	12.178	53.959	65.713	143.06
Milk + AO7	10.328	13.721	13.721	67.523	68.537	121.03
Cheese water + AO7	10.328	18.834	51.858	57.447	97.339	101.89

Nyquist plots, the imaginary component of the impedance is plotted against its real component with decreasing frequencies (Barsoukov and Macdonald 2005; Yuan et al. 2010; Dominguez-Benetton et al. 2012). The solution conductivity and the interaction between electrode and solution are important parameters affecting R_s value. R_{ct} depends on the electrode conductivity and appears as a semicircle arc in high frequencies, where its diameter determines the R_{ct} value. The Warburg resistance, caused by mass transfer diffusion, is recognizable by a line at an angle of 45° in the low-frequency area (Varanasi et al. 2016; Gupta et al. 2017). In this work, EIS was performed in a 10 mM $K_3[Fe(CN)_6]/K_4[Fe(CN)_6]$ + 0.1 M KCl solution and in the anolyte solution of the MFC as well. The results are presented as Nyquist plots and their equivalent circuits were elicited via EIS Spectrum Analyzer® software (Fig. 7a, b). The R_s, R_{ct}, and W values are displayed in Table 4 based on the equivalent circuits drawn out in Fig. 7 as R_1, R_2, and W_1, respectively. According to Fig. 7b and Table 4, the amounts of R_1, R_2, and W_1 decreased significantly for the biofilm-coated electrodes compared with the bare graphite in the anolyte solution of MFC. The R_s values should be the same for all the electrodes immersed in the same solution; nevertheless, the biofilm-coated electrodes have fewer values due to the less resistance in electrode–solution interfaces (Modi et al. 2016). Biofilm formation can accelerate and catalyze the electron transfer to the anode and reduce its overpotential (Mehdinia et al. 2014; Varanasi et al. 2016).

Conclusion

In this study, the application of MFC technology for the simultaneous electrical energy production and the treatment of the mixture of dairy products and dye solution was investigated. The results show that by using the dairy by-products as the co-substrate of the anolyte, a biofilm with rod-shaped microorganisms successfully coats the anode surface. Considering the CV graphs, the redox peaks and high current values are obvious for yogurt water + AO7 and milk + AO7 MFCs confirming their high electrochemical activity. Cheese water + AO7 and milk + AO7 MFCs exhibit high COD removal and decolorization efficiencies. Cheese water + AO7 MFC shows the maximum power density and voltage output, while milk + AO7 MFC possesses a more stable voltage. The power density and the voltage of milk + AO7 MFC are very close to cheese water + AO7 MFC. According to the findings of this work, AO7 decolorization and electricity production are successfully achievable in the presence of dairy by-products.

Acknowledgments This research was performed in the Research Laboratory of Environmental Protection Technology (RLEPT) of the University of Tabriz with the support of the central laboratory and other sections and also financial help of the university. The authors would like to appreciate all the support received from the University of Tabriz.

References

Abdollahi B, Shakeri A, Aber S, Sharifi Bonab M (2018) Simultaneous photodegradation of acid orange 7 and removal of Pb2+ from polluted water using reusable clinoptilolite–TiO2 nanocomposite. Res Chem Intermed 44:1505–1521. https://doi.org/10.1007/s11164-017-3181-3

Barsoukov E, Macdonald JR (eds) (2005) Impedance spectroscopy: theory, experiment, and applications, 2nd edn. Wiley-Interscience, Hoboken

Burkitt R, Whiffen TR, Yu EH (2016) Iron phthalocyanine and MnOx composite catalysts for microbial fuel cell applications. Appl Catal B Environ 181:279–288. https://doi.org/10.1016/j.apcatb.2015.07.010

Cao X, Wang H, Li X, Fang Z, Li XN (2017) Enhanced degradation of azo dye by a stacked microbial fuel cell-biofilm electrode reactor coupled system. Bioresour Technol 227:273–278. https://doi.org/10.1016/j.biortech.2016.12.043

Chen B-Y, Zhang M-M, Ding Y, Chang C-T (2010) Feasibility study of simultaneous bioelectricity generation and dye decolorization using naturally occurring decolorizers. J Taiwan Inst Chem Eng 41:682–688. https://doi.org/10.1016/j.jtice.2010.02.005

Chen W, Liu Z, Hou J, Zhou Y, Lou X, Li Y (2018) Enhancing performance of microbial fuel cells by using novel double-layer-capacitor-materials modified anodes. Int J Hydrog Energy 43:1816–1823. https://doi.org/10.1016/j.ijhydene.2017.11.034

Choi Y-J, Jung E-K, Park H-J et al (2007) Effect of initial carbon sources on the performance of a microbial fuel cell containing environmental microorganism Micrococcus luteus. Bull Kor Chem Soc 28:1591–1594

Cirik K (2014) Optimization of bioelectricity generation in fed-batch microbial fuel cell: effect of electrode material, initial substrate concentration, and cycle time. Appl Biochem Biotechnol 173:205–214. https://doi.org/10.1007/s12010-014-0834-1

Dominguez-Benetton X, Sevda S, Vanbroekhoven K, Pant D (2012) The accurate use of impedance analysis for the study of microbial electrochemical systems. Chem Soc Rev 41:7228–7246. https://doi.org/10.1039/c2cs35026b

Fang Z, Cheng S, Wang H, Cao X, Li X (2017) Feasibility study of simultaneous azo dye decolorization and bioelectricity generation by microbial fuel cell-coupled constructed wetland: substrate effects. RSC Adv 7:16542–16552. https://doi.org/10.1039/C7RA01255A

Faria A, Gonçalves L, Peixoto JM, Peixoto L, Brito AG, Martins G (2017) Resources recovery in the dairy industry: bioelectricity production using a continuous microbial fuel cell. J Clean Prod 140:971–976. https://doi.org/10.1016/j.jclepro.2016.04.027

Fernando E, Keshavarz T, Kyazze G (2012) Enhanced bio-decolourisation of acid orange 7 by Shewanella oneidensis through co-metabolism in a microbial fuel cell. Int Biodeterior Biodegrad 72:1–9. https://doi.org/10.1016/j.ibiod.2012.04.010

Fernando E, Keshavarz T, Kyazze G (2014a) Complete degradation of the azo dye acid orange-7 and bioelectricity generation in an integrated microbial fuel cell, aerobic two-stage bioreactor system in continuous flow mode at ambient temperature. Bioresour Technol 156:155–162. https://doi.org/10.1016/j.biortech.2014.01.036

Fernando E, Keshavarz T, Kyazze G (2014b) External resistance as a potential tool for influencing azo dye reductive decolourisation kinetics in microbial fuel cells. Int Biodeterior Biodegrad 89:7–14. https://doi.org/10.1016/j.ibiod.2013.12.011

Galai S, Pérez de los Ríos A, Hernández-Fernández FJ et al (2015) Microbial fuel cell application for azoic dye decolorization with simultaneous bioenergy production using *Stenotrophomonas* sp. Chem Eng Technol 38:1511–1518. https://doi.org/10.1002/ceat.201400608

Garino N, Sacco A, Castellino M, Muñoz-Tabares JA, Chiodoni A, Agostino V, Margaria V, Gerosa M, Massaglia G, Quaglio M (2016) Microwave-assisted synthesis of reduced graphene oxide/SnO_2 nanocomposite for oxygen reduction reaction in microbial fuel cells. ACS Appl Mater Interfaces 8:4633–4643. https://doi.org/10.1021/acsami.5b11198

Ge Z, Li J, Xiao L, Tong, Y, He Z (2014) Recovery of electrical energy in microbial fuel cells: brief review. Environ Sci Tech Let 1(2):137–141. https://doi.org/10.1021/ez4000324

Gupta S, Yadav A, Singh S, Verma N (2017) Synthesis of silicon carbide-derived carbon as an electrode of a microbial fuel cell and an adsorbent of aqueous Cr(VI). Ind Eng Chem Res 56:1233–1244. https://doi.org/10.1021/acs.iecr.6b03832

Harnisch F, Freguia S (2012) A basic tutorial on cyclic voltammetry for the investigation of electroactive microbial biofilms. Chem Asian J 7:466–475. https://doi.org/10.1002/asia.201100740

Hassan AN, Nelson BK (2012) Invited review: anaerobic fermentation of dairy food wastewater. J Dairy Sci 95:6188–6203. https://doi.org/10.3168/jds.2012-5732

Hassan M, Pous N, Xie B, Colprim J, Balaguer MD, Puig S (2017) Influence of iron species on integrated microbial fuel cell and electro-Fenton process treating landfill leachate. Chem Eng J 328:57–65. https://doi.org/10.1016/j.cej.2017.07.025

Hindatu Y, Annuar MSM, Gumel AM (2017) Mini-review: anode modification for improved performance of microbial fuel cell. Renew Sust Energ Rev 73:236–248. https://doi.org/10.1016/j.rser.2017.01.138

Holkar CR, Arora H, Halder D, Pinjari DV (2018) Biodegradation of reactive blue 19 with simultaneous electricity generation by the newly isolated electrogenic Klebsiella sp. C NCIM 5546 bacterium in a microbial fuel cell. Int Biodeterior Biodegrad 133:194–201. https://doi.org/10.1016/j.ibiod.2018.07.011

Holkar CR, Jadhav AJ, Pinjari DV, Mahamuni NM, Pandit AB (2016) A critical review on textile wastewater treatments: possible approaches. J Environ Manag 182:351–366. https://doi.org/10.1016/j.jenvman.2016.07.090

Hsueh C-C, Wang Y-M, Chen B-Y (2014) Metabolite analysis on reductive biodegradation of reactive green 19 in Enterobacter cancerogenus bearing microbial fuel cell (MFC) and non-MFC cultures. J Taiwan Inst Chem Eng 45:436–443. https://doi.org/10.1016/j.jtice.2013.05.003

Huang L, Li X, Ren Y, Wang X (2016) In-situ modified carbon cloth with polyaniline/graphene as anode to enhance performance of microbial fuel cell. Int J Hydrog Energy 41:11369–11379. https://doi.org/10.1016/j.ijhydene.2016.05.048

Islam MA, Ethiraj B, Cheng CK, Yousuf A, Thiruvenkadam S, Prasad R, Rahman Khan MM (2018) Enhanced current generation using mutualistic interaction of yeast-bacterial coculture in dual chamber microbial fuel cell. Ind Eng Chem Res 57:813–821. https://doi.org/10.1021/acs.iecr.7b01855

Ismail ZZ, Habeeb AA (2017) Experimental and modeling study of simultaneous power generation and pharmaceutical wastewater treatment in microbial fuel cell based on mobilized biofilm bearers. Renew Energy 101:1256–1265. https://doi.org/10.1016/j.renene.2016.10.008

Jadhav DA, Deshpande PA, Ghangrekar MM (2017) Enhancing the performance of single-chambered microbial fuel cell using manganese/palladium and zirconium/palladium composite cathode catalysts. Bioresour Technol 238:568–574. https://doi.org/10.1016/j.biortech.2017.04.085

Jegatheesan V, Pramanik BK, Chen J, Navaratna D, Chang CY, Shu L (2016) Treatment of textile wastewater with membrane bioreactor: a critical review. Bioresour Technol 204:202–212. https://doi.org/10.1016/j.biortech.2016.01.006

Karadag D, Koroglu OE, Ozkaya B, Cakmakci M, Heaven S, Banks C, Serna-Maza A (2015a) Anaerobic granular reactors for the treatment of dairy wastewater: a review. Int J Dairy Technol 68:459–470. https://doi.org/10.1111/1471-0307.12252

Karadag D, Köroğlu OE, Ozkaya B, Cakmakci M (2015b) A review on anaerobic biofilm reactors for the treatment of dairy industry wastewater. Process Biochem 50:262–271. https://doi.org/10.1016/j.procbio.2014.11.005

Kardi SN, Ibrahim N, Rashid NAA, Darzi GN (2016) Simultaneous acid red 27 decolourisation and bioelectricity generation in a (H-type) microbial fuel cell configuration using NAR-2. Environ Sci Pollut Res 23:3358–3364. https://doi.org/10.1007/s11356-015-5538-8

Katheresan V, Kansedo J, Lau SY (2018) Efficiency of various recent wastewater dye removal methods: a review. J Environ Chem Eng 6:4676–4697. https://doi.org/10.1016/j.jece.2018.06.060

Khan MD, Khan N, Sultana S, Joshi R, Ahmed S, Yu E, Scott K, Ahmad A, Khan MZ (2017) Bioelectrochemical conversion of waste to energy using microbial fuel cell technology. Process Biochem 57:141–158. https://doi.org/10.1016/j.procbio.2017.04.001

Kim BH, Park HS, Kim HJ, Kim GT, Chang IS, Lee J, Phung NT (2004) Enrichment of microbial community generating electricity using a fuel-cell-type electrochemical cell. Appl Microbiol Biotechnol 63:672–681. https://doi.org/10.1007/s00253-003-1412-6

Kim GT, Webster G, Wimpenny JWT, Kim BH, Kim HJ, Weightman AJ (2006) Bacterial community structure, compartmentalization and activity in a microbial fuel cell. J Appl Microbiol 101:698–710. https://doi.org/10.1111/j.1365-2672.2006.02923.x

Lai C-Y, Wu C-H, Meng C-T, Lin C-W (2017) Decolorization of azo dye and generation of electricity by microbial fuel cell with laccase-producing white-rot fungus on cathode. Appl Energy 188:392–398. https://doi.org/10.1016/j.apenergy.2016.12.044

Liu X-W, Huang Y-X, Sun X-F, Sheng GP, Zhao F, Wang SG, Yu HQ (2014) Conductive carbon nanotube hydrogel as a bioanode for enhanced microbial electrocatalysis. ACS Appl Mater Interfaces 6:8158–8164. https://doi.org/10.1021/am500624k

Logan BE (2008) Microbial fuel cells. Wiley-Interscience, Hoboken

Logan BE, Hamelers B, Rozendal R, Schröder U, Keller J, Freguia S, Aelterman P, Verstraete W, Rabaey K (2006) Microbial fuel cells: methodology and technology. Environ Sci Technol 40:5181–5192. https://doi.org/10.1021/es0605016

Mani P, Keshavarz T, Chandra TS, Kyazze G (2017a) Decolourisation of acid orange 7 in a microbial fuel cell with a laccase-based biocathode: influence of mitigating pH changes in the cathode chamber. Enzym Microb Technol 96:170–176. https://doi.org/10.1016/j.enzmictec.2016.10.012

Mani P, Keshavarz T, Chandra TS, Kyazze G (2017b) Decolourisation of acid orange 7 in a microbial fuel cell with a laccase-based biocathode: influence of mitigating pH changes in the cathode chamber. Enzym Microb Technol 96:170–176. https://doi.org/10.1016/j.enzmictec.2016.10.012

Mehdinia A, Ziaei E, Jabbari A (2014) Multi-walled carbon nanotube/SnO2 nanocomposite: a novel anode material for microbial fuel cells. Electrochim Acta 130:512–518. https://doi.org/10.1016/j.electacta.2014.03.011

Miran W, Nawaz M, Jang J, Lee DS (2016) Sustainable electricity generation by biodegradation of low-cost lemon peel biomass in a dual chamber microbial fuel cell. Int Biodeterior Biodegrad 106:75–79. https://doi.org/10.1016/j.ibiod.2015.10.009

Miran W, Nawaz M, Kadam A, Shin S, Heo J, Jang J, Lee DS (2015) Microbial community structure in a dual chamber microbial fuel cell fed with brewery waste for azo dye degradation and electricity

generation. Environ Sci Pollut Res 22:13477–13485. https://doi.org/10.1007/s11356-015-4582-8

Modi A, Singh S, Verma N (2016) In situ nitrogen-doping of nickel nanoparticle-dispersed carbon nanofiber-based electrodes: its positive effects on the performance of a microbial fuel cell. Electrochim Acta 190:620–627. https://doi.org/10.1016/j.electacta.2015.12.191

Pasupuleti SB, Srikanth S, Dominguez-Benetton X, Mohan SV, Pant D (2016) Dual gas diffusion cathode design for microbial fuel cell (MFC): optimizing the suitable mode of operation in terms of bioelectrochemical and bioelectro-kinetic evaluation: dual gas diffusion cathode design for microbial fuel cell (MFC). J Chem Technol Biotechnol 91:624–639. https://doi.org/10.1002/jctb.4613

Penteado ED, Fernandez-Marchante CM, Zaiat M, Gonzalez ER, Rodrigo MA (2017) Influence of carbon electrode material on energy recovery from winery wastewater using a dual-chamber microbial fuel cell. Environ Technol 38:1333–1341. https://doi.org/10.1080/09593330.2016.1226961

Rice EW, Baird RB, Eaton AD (2017) Standard methods for the examination of water and wastewater, 23rd edn. American Public Health Association

Rikame SS, Mungray AA, Mungray AK (2012) Electricity generation from acidogenic food waste leachate using dual chamber mediator less microbial fuel cell. Int Biodeterior Biodegrad 75:131–137. https://doi.org/10.1016/j.ibiod.2012.09.006

Samsudeen N, Radhakrishnan TK, Matheswaran M (2015) Bioelectricity production from microbial fuel cell using mixed bacterial culture isolated from distillery wastewater. Bioresour Technol 195:242–247. https://doi.org/10.1016/j.biortech.2015.07.023

Savizi ISP, Kariminia H-R, Bakhshian S (2012) Simultaneous decolorization and bioelectricity generation in a dual chamber microbial fuel cell using electropolymerized-enzymatic cathode. Environ Sci Technol 46:6584–6593. https://doi.org/10.1021/es300367h

Schröder U (2007) Anodic electron transfer mechanisms in microbial fuel cells and their energy efficiency. Phys Chem Chem Phys 9:2619–2629. https://doi.org/10.1039/B703627M

Shin J-W, Song Y-H, An B-M, Seo SJ, Park JY (2014) Energy recovery of ethanolamine in wastewater using an air-cathode microbial fuel cell. Int Biodeterior Biodegrad 95:117–121. https://doi.org/10.1016/j.ibiod.2014.05.021

Su CX-H, Low LW, Teng TT, Wong YS (2016) Combination and hybridisation of treatments in dye wastewater treatment: a review. J Environ Chem Eng 4:3618–3631. https://doi.org/10.1016/j.jece.2016.07.026

Sun Z, Cao R, Huang M, Chen D, Zheng W, Lin L (2015) Effect of light irradiation on the photoelectricity performance of microbial fuel cell with a copper oxide nanowire photocathode. J Photochem Photobiol A Chem 300:38–43. https://doi.org/10.1016/j.jphotochem.2014.12.003

Thung W-E, Ong S-A, Ho L-N, Wong YS, Ridwan F, Lehl HK, Oon YL, Oon YS (2018) Biodegradation of acid orange 7 in a combined anaerobic-aerobic up-flow membrane-less microbial fuel cell: mechanism of biodegradation and electron transfer. Chem Eng J 336:397–405. https://doi.org/10.1016/j.cej.2017.12.028

Varanasi JL, Nayak AK, Sohn Y, Pradhan D, Das D (2016) Improvement of power generation of microbial fuel cell by integrating tungsten oxide electrocatalyst with pure or mixed culture biocatalysts. Electrochim Acta 199:154–163. https://doi.org/10.1016/j.electacta.2016.03.152

Venkata Mohan S, Mohanakrishna G, Velvizhi G, Babu VL, Sarma PN (2010) Bio-catalyzed electrochemical treatment of real field dairy wastewater with simultaneous power generation. Biochem Eng J 51:32–39. https://doi.org/10.1016/j.bej.2010.04.012

Wang G, Wei L, Cao C, Su M, Shen J (2017) Novel resolution-contrast method employed for investigating electron transfer mechanism of the mixed bacteria microbial fuel cell. Int J Hydrog Energy 42:11614–11621. https://doi.org/10.1016/j.ijhydene.2017.02.029

Wang H, Luo H, Fallgren PH, Jin S, Ren ZJ (2015) Bioelectrochemical system platform for sustainable environmental remediation and energy generation. Biotechnol Adv 33:317–334. https://doi.org/10.1016/j.biotechadv.2015.04.003

Wong NP (ed) (1988) Fundamentals of dairy chemistry, 3rd edn. Van Nostrand Reihold Co, New York

Yuan G-E, Li Y, Lv J, Zhang G, Yang F (2017) Integration of microbial fuel cell and catalytic oxidation reactor with iron phthalocyanine catalyst for Congo red degradation. Biochem Eng J 120:118–124. https://doi.org/10.1016/j.bej.2017.01.005

Yuan X-Z, Song C, Wang H, Zhang J (2010) Electrochemical impedance spectroscopy in PEM fuel cells. Springer, London

Zhao F, Slade RCT, Varcoe JR (2009) Techniques for the study and development of microbial fuel cells: an electrochemical perspective. Chem Soc Rev 38:1926–1939. https://doi.org/10.1039/b819866g

Zhao N, Angelidaki I, Zhang Y (2017) Electricity generation and microbial community in response to short-term changes in stack connection of self-stacked submersible microbial fuel cell powered by glycerol. Water Res 109:367–374. https://doi.org/10.1016/j.watres.2016.11.064